PHYSICAL REVIEW B **74**, 241104(R) (2006)

Metal-insulator transition in $Ca_{1-x}Na_xIrO_3$ with post-perovskite structure

K. Ohgushi, H. Gotou, T. Yagi, Y. Kiuchi, F. Sakai, and Y. Ueda
Institute for Solid State Physics, University of Tokyo, Kashiwa, Chiba 277-8581, Japan
(Received 13 November 2006; published 20 December 2006)

We develop a solid solution $Ca_{1-x}Na_xIrO_3$ ($0 \leqslant x \leqslant 0.37$), which exhibits a filling-control metal-insulator transition on a quasi-two-dimensional lattice. The carrier doping into the $S=1/2$ antiferromagnetic Mott insulator $CaIrO_3$ destabilizes the magnetic long-range order, culminating in a paramagnetic state at $x>0.30$, with simultaneous change from insulating to metallic behavior. The temperature (T) dependence of the resistivity for metallic samples ($0.31 \leqslant x \leqslant 0.37$) exhibits several characteristic features: (1) a T^{α} dependence with $\alpha \sim 1.2$ in a metallic range, (2) ln T dependence in a weak-localization regime, and (3) positive magnetoresistance violating Kohler's rule. These observations offer a solid foundation to unravel anomalous properties in the normal state of high-T_c cuprates.

DOI: 10.1103/PhysRevB.74.241104 PACS number(s): 71.30.+h, 72.15.Rn, 73.43.Nq, 74.25.Fy

The metal-insulator transition (MIT) arising from electron correlation effects is a central topic in condensed matter physics,[1] not only because superconductivity appears on the verge of the MIT in high-T_c cuprates,[2] but also because the critical behavior of the MIT and the nature of the correlated metallic state are fundamental issues. Considerable attention has focused on quasi-two-dimensional MIT systems with a small spin quantum number, where a long-range magnetic order is suppressed by large quantum fluctuations even in the insulating limit. Physical realizations include $Ca_{2-x}Sr_xRuO_4$,[3] κ-$(BEDT\text{-}TTF)_2Cu[N(CN)_2]Cl$,[4] $La_{2-x}Sr_xNiO_4$,[5,6] and $Sr_{2-x}La_xVO_4$,[7] the former two being categorized into the bandwidth-control system, whereas the latter two are rare examples of the filling-control system. It is required to uncover universality as well as material characteristics concerning the MIT by studying various systems.

$CaIrO_3$ with *Cmcm* orthorhombic symmetry[8–10] has captured great geophysical interest, since isostructural $MgSiO_3$ is considered to be a main constituent of the D'' region in the lowermost mantle.[11–14] The crystal structure (right inset of Fig. 1), which is now called the post-perovskite structure, comprises IrO_3 layers and eightfold-coordinated Ca^{2+} ions in between.[15] Within each plane, IrO_6 octahedra are connected with each other by sharing edges and corners along the a and c axes, respectively, giving rise to a rectangular lattice of Ir^{4+} ions with the t_{2g}^5 electron configuration ($S=1/2$). The purpose of the present Rapid Communication is to report electronic properties of Na-substituted $CaIrO_3$. We show that this system exhibits a genetic MIT with a simultaneous change of a magnetic ground state from an antiferromagnetic (AF) to a paramagnetic state. The non-Fermi-liquid behavior manifests itself through the analysis of (magneto)resistance for metallic samples.

Polycrystalline $Ca_{1-x}Na_xIrO_3$ ($0 \leqslant x \leqslant 0.37$) was prepared by using a cubic-anvil-type high-pressure apparatus.[16] CaO, Na_2O_2, and IrO_2 were mixed and packed into a Pt capsule 3.0 mm in length and 5.5 mm in diameter in a glove box. In order to make a sample without remaining IrO_2, it was important to add excess of CaO and Na_2O_2 to the stoichiometric amounts. The IrO_2 phase precluded collecting reliable data for $0.37 < x < 0.65$. The synthesis temperature was smoothly varied as a function of Na content (x) from 1150 °C for $x=0$ to 800 °C for $x=0.37$, while the synthesis pressure was kept 4 GPa for all x. The obtained polycrystals were characterized by a powder x-ray diffraction using Cu $K\alpha$ radiation. The lattice parameters of $CaIrO_3$ are estimated to be $a=3.147(1)$ Å, $b=9.863(2)$ Å, and $c=7.299(1)$ Å. With an increase in x, the unit cell is elongated along the layer direction (the b axis), being the same characteristics as hole-doped high-T_c cuprates. By plotting lattice parameters against x determined by a scanning electron microscope (SEM) equipped with an energy-dispersive x-ray (EDX) spectrometer, we found linear relations (Vegard's law) such as $a=3.148-0.117x$, $b=9.861+0.368x$, and $c=7.303-0.066x$ in units of Å. We deduce the x value of the samples investigated here by substituting lattice parameters

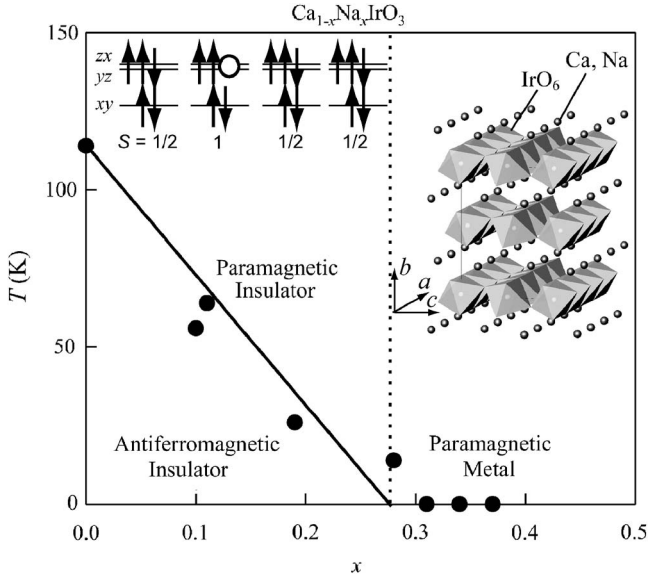

FIG. 1. The electronic phase diagram for $Ca_{1-x}Na_xIrO_3$ ($0 \leqslant x \leqslant 0.37$) within a temperature-Na content (T-x) plane. Left inset: schematic view of the electron configuration among the t_{2g} orbitals, d_{xy}, d_{yz}, and d_{zx}, with x, y, and z being the local coordinate axes at the Ir site. One doped carrier denoted by an open circle forms a triplet (high-spin) state with the preexisting carrier. Right inset: post-perovskite structure composed of IrO_3 layers and Ca^{2+} and Na^+ ions in between.

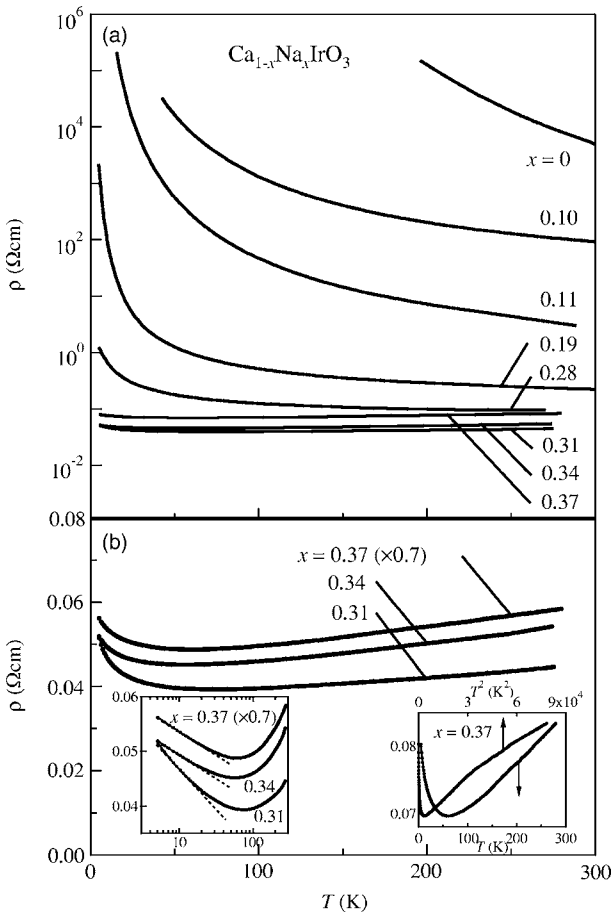

FIG. 2. (a) The temperature (T) dependence of the resistivity (ρ) for $Ca_{1-x}Na_xIrO_3$ ($0 \leqslant x \leqslant 0.37$) in a logarithmic ordinate scale. (b) The ρ curves for $x=0.31$, 0.34, and 0.37 in a linear ordinate scale. Note that the data for $x=0.37$ are multiplied by 0.7 for clarification. The left inset shows the same data on a logarithmic abscissa scale. The dotted lines are guides to the eyes. The right inset plots ρ for $x=0.37$ against T and T^2.

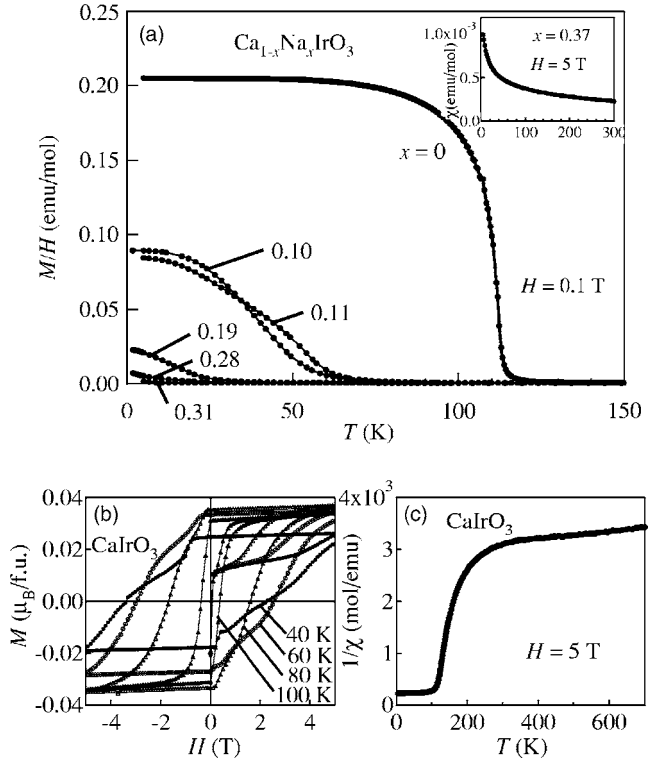

FIG. 3. (a) The magnetization divided by the external magnetic field (M/H) at $H=0.1$ T for $Ca_{1-x}Na_xIrO_3$ ($0 \leqslant x \leqslant 0.37$) as a function of temperature (T). The measurements were performed during the cooling process. The inset shows $\chi=M/H$ for $x=0.37$ at 5 T in a extended T range ($0<T<300$ K). (b) Isothermal magnetization curves for $CaIrO_3$ at various Ts. (c) Curie-Weiss plot of χ for $CaIrO_3$ in $0<T<700$ K.

into these formulas. The resistivity was measured by a standard four-probe technique with special care not to expose highly hygroscopic Na-doped compounds to air. We covered the sample with vacuum grease in a glove box after attaching copper wires to the sample with silver paste. The magnetoresistance was measured in a transverse geometry, where the external magnetic field is perpendicular to the current direction. The magnetization measurements were performed with use of a commercial superconducting quantum interference device (SQUID) magnetometer.

We first focus on the undoped compound ($x=0$). The resistivity (ρ) shown in Fig. 2(a) follows well the Arrhenius-type temperature (T) dependence, $\rho(T)=A\exp(\Delta/T)$, with the activation energy (Δ) of 0.17 eV, indicating that $CaIrO_3$ is a Mott insulator. This compound undergoes an AF transition at 115 K ($=T_N$), which is unambiguously evaluated by the parasitic ferromagnetism reaching $0.037\mu_B$/Ir at 5 K [Fig. 3(a)]. As can be clearly seen from Fig. 3(b), isothermal magnetization curves exhibit a large hysteresis, making a reverse of magnetization (M) by the external magnetic field (H) impossible below 40 K. This infers that Ir^{4+} spins are strongly anisotropic. Figure 3(c) represents $1/\chi$ ($=H/M$) as a function of T. The deviation from the linear behavior at considerably high T ($\sim$350 K) evidences the development of AF correlations far above T_N—in other word, the suppression of T_N by some reasons such as the low dimensionality and/or the smallness of the spin quantum number ($S=1/2$). The Curie-Weiss fit to χ above 400 K yields a Curie-Weiss temperature (θ_{CW}) of 3900 K with an unphysically large effective magnetic moment $p=3.29$. When fitting the same data to a Curie-Weiss term with fixed $p=1.73$ (theoretical value for $S=1/2$) plus a T-independent term (χ_0), we obtain $\theta_{CW}=1800$ K and $\chi_0=1.4\times10^{-4}$ emu/mol. These results suggest a large exchange integral (J) of, at least, several hundred K and sizable contributions from orbital magnetic moments.

These features can be partly interpreted by considering the local environment of Ir^{4+} ions. In the post-perovskite structure, four of six O^{2-} ions coordinating an Ir^{4+} ion participate in the edge-sharing bond with the longer Ir-O distance; therefore, there is a crystal field splitting between the lower d_{xy} orbital and the upper d_{zx} and d_{yz} orbitals, where x, y, and z are the local coordinate axes with the z axis along the corner-sharing direction. When one hole occupies the twofold-degenerated d_{zx} and d_{yz} orbitals, the strong spin-orbit coupling in the 5d transition metal atoms most likely stabilizes a certain complex orbital order with an unquenched orbital magnetic moment—say, $d_{zx}\pm id_{yz}$. The thus

generated huge single-ion anisotropies, together with the difference in the local principal axis among adjacent IrO_6 octahedra (right inset of Fig. 1), cause the canted spin state with the weak ferromagnetism.

Figures 2(a) and 2(b) show the T dependence of ρ for $Ca_{1-x}Na_xIrO_3$ ($0 \leqslant x \leqslant 0.37$), clearly demonstrating the MIT between $x=0.28$ and 0.31. Here, we note that the ρ basically corresponds to the in-plane resistivity, because the electrons are expected to be more conducting within the a-c planes owing to the layered structure. The values of ρ systematically become larger with increasing x in a metallic regime ($0.31 \leqslant x \leqslant 0.37$); this probably corresponds to the fact that degradation of samples by absorbing waters is accelerated with an increase in x. As can be seen from Fig. 3(a), upon carrier doping, T_N gradually decreases until a paramagnetic state down to the lowest T measured is eventually achieved at $x=0.31$. From these data, we draw an electronic phase diagram depicted in Fig. 1. The present system shows a transition from an AF insulator to a paramagnetic metal without an intervening AF metallic phase, markedly contrasting with many MIT systems in three dimensions.[1] Instead, the absence of AF metallic state resembles high-T_c cuprates with a quasi-two-dimensional lattice, implying that the dimensionality is the key to the topology of the phase diagram. The attempt to synthesize Y^{3+}-substituted compounds in a single phase form was abandoned due to the appearance of the pyrochlore phase; however, magnetization experiments indicate $T_N \sim 50$ K in $Ca_{1-x}Y_xIrO_3$ with $x=0.06$ (data not shown), an abrupt decrease in T_N compared with the Na^+-substituted case. This particle-hole asymmetry resides in the coupling manner between a doped carrier and the preexisting $S=1/2$ spin in doubly degenerated d_{zx} and d_{yz} orbitals. When Ca^{2+} ions are partially replaced by Y^{3+} ions, the doped electron has an antiparallel alignment with the preexisting spin, giving rise to a spin singlet ($S=0$) state. On the contrary, the extra hole produced by the Na^+ substitution forms a spin-triplet (high-spin) state; the resultant local $S=1$ spin continues to retain the AF state against the tendency of mobile carriers to destroy the AF order. This situation is in stark contrast to high-T_c cuprates, where a Zhang-Rice singlet is formed, irrespective of the type of carriers, owing to the single band nature.[17]

We discuss the precise T dependence of ρ in the AF insulating phase ($0 \leqslant x \leqslant 0.28$). While the Arrhenius-type behavior ($\nu=1$ in the below function) well describes the T dependence of ρ for $x=0$, the ρ curves for carrier-doped samples very weakly diverge; we estimate the extent of divergence by ν (=1, 2, 3, and 4), with which $\rho(T)=A\exp(T_0/T)^{1/\nu}$ (A and T_0 being suitable constants) describes experimental curves in the widest T range. The evaluated ν is 2 for $x=0.10$ ($T<160$ K), 3 for $x=0.11$ ($T<70$ K) and 0.19 ($T<18$ K), and 4 for $x=0.28$ ($T<8$ K); $\nu=2$, 3, and 4, respectively, correspond to the variable range hopping (VRH) conduction in one, two, and three dimensions.[18] This crossover from Mott insulating ($\nu=1$) to VRH ($\nu=2$, 3, and 4) behavior is also observed in $Ca_{2-x}Sr_xRuO_4$ and argued in terms of the disorder-modified Mott gap.[19] Our results indicate that, as far as the disorder effects are concerned, there is no essential difference between the bandwidth- and filling-control systems.

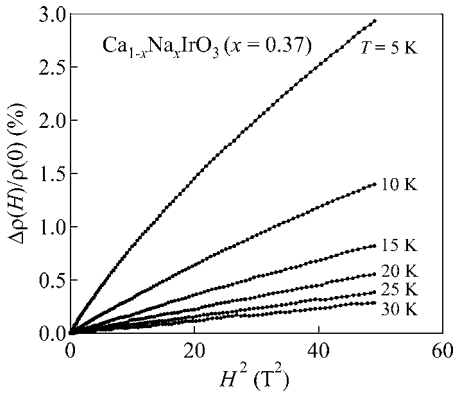

FIG. 4. The transverse magnetoresistance $\Delta\rho(H)/\rho(0) = [\rho(H)-\rho(0)]/\rho(0)$ for $Ca_{1-x}Na_xIrO_3$ ($x=0.37$) plotted against the square of the external magnetic field (H).

Even in the metallic phase ($0.31 \leqslant x \leqslant 0.37$), there is a T range of $d\rho/dT<0$ (typically $T<50$ K). This increase in ρ follows neither $\rho(T) \propto \exp(T_0/T)^{1/\nu}$ nor $\rho(T) \propto 1/T^{1/2}$; instead, as shown in the left inset of Fig. 2(b), the ρ curve exhibits the $\ln T$ divergence, being attributable to the weak localization in two-dimensions with electron correlation effects.[20] We remark that the $\ln T$ divergence is also discerned in the underdoped high-T_c cuprates under the strong magnetic field.[21]

We now turn our attention to the $d\rho/dT>0$ range of metallic compounds. By plotting ρ for $x=0.37$ against T^2 [the right inset of Fig. 2(b)], we see that the present compound is beyond the description of the Fermi liquid theory; the fit of ρ above 100 K with the form $\rho(T)=\rho_0+AT^\alpha$ yields $\alpha=1.2$, deviating from 2 expected for Fermi liquid. This type of deviation is often observed in correlated metals near magnetic instabilities, where magnetic fluctuations are critically enhanced.[1] In the present system, AF fluctuations can be monitored by χ at $\vec{q}=0$ ($\vec{q}$ being the wave number), because the weak ferromagnetic moment ($\vec{q}=0$ component) is parasitic on the antiferromagnetically ordered ($\vec{q} \neq 0$) state. The monotonous increase in χ for $x=0.37$ with decreasing T [inset of Fig. 3(a)], corresponding to the deviation from the Curie-Weiss behavior below 350 K in $x=0$, persuasively evidences the presence of AF fluctuations in this composition. The mode-mode coupling theory predicts $\alpha=1$ for the two-dimensional metal with AF fluctuations,[22] being slightly smaller than the experimentally observed α. The reason for this discrepancy is unclear at present.

Figure 4 represents the magnetoresistance $\Delta\rho/\rho$ $[=\rho(T,H)/\rho(T,0)-1]$ for $x=0.37$ in a transverse geometry. The $\Delta\rho/\rho$ obeys the H^2 dependence and reaches 2.9% at 5 K and 7 T. The positive magnetoresistance is incompatible with the H-induced suppression of the interference effect associated with the weak localization and, instead, is in accordance with the orbital magnetoresistance. In a conventional metal, the T dependence of the orbital magnetoresistance can be pushed into the T dependence of $\rho(T,0)$ in such a way that $\Delta\rho/\rho=F(H/\rho(T,0))$, where F is a material-dependent function and is usually taken as $F(x)=x^2$; this Kohler's rule is deduced from Boltzmann transport equations.[23] However, the plots of $\Delta\rho/\rho$ for $x=0.37$ against $[H/\rho(T,0)]^2$ for various

T's do not overlap with each other, even after subtracting a contribution from the weak localization effect from $\rho(T,0)$ in advance; the T dependence of $\Delta\rho/\rho$ is too abrupt compared with that of $\rho(T,0)$. Kohler's rule is also violated in underdoped high-T_c cuprates;[24] this, together with the T^2 dependence of the cotangent of the Hall angle (θ_H), builds the solid foundations of introducing two scattering rates τ_{tr} and τ_H.[25] Unusual magnetotransport properties in high-T_c cuprates are theoretically discussed in term of the non-Fermi liquid,[26] the pseudogap state,[27] and so on. Violation of Kohler's rule in $Ca_{1-x}Na_xIrO_3$ offers a good testing ground for these theories; however, more information on electronic and magnetic properties for this system is needed for identifying the origin of anomalous magnetotransport properties of the correlated metallic state on the verge of MIT in two dimensions.

We summarize this Rapid Communication by comparing $Ca_{1-x}Na_xIrO_3$ ($0 \leqslant x \leqslant 0.37$) with the hole-doped high-T_c cuprates. There are many similarities between two systems. The parent compounds are $S=1/2$ AF Mott insulator on the quasi-two-dimensional lattice. Upon carrier doping, the AF order is gradually destroyed into the paramagnetic metallic state. The correlated metallic state near the MIT boundary is beyond the simple Fermi liquid, as evidenced by the T^α dependence of ρ with $\alpha < 2$ as well as the violation of Kohler's rule. The weak localization in two dimensions characterized by the $\ln T$ dependence governs the ρ in the low-T ranges. On the other hand, there are several differences. The most crucial one is whether superconductivity appears or not in the vicinity of the MIT. From the viewpoint of electronic structures, this involves how a doped carrier couples with the original spin. The singlet coupling as formed in high-T_c cuprates drives the superconducting instability, whereas the triplet coupling in $Ca_{1-x}Na_xIrO_3$ merely renders the system metallic. This is also relevant to the difference in the critical concentration (x_c) of the MIT: the small $x_c(\sim 0.1)$ in high-T_c cuprates and the large $x_c(\sim 0.3)$ in $Ca_{1-x}Na_xIrO_3$. The nature of spins in parent compounds is also distinguishable. While high-T_c cuprates have Heisenberg spins in the e_g orbitals, spins in $CaIrO_3$ are strongly anisotropic, reflecting the prominence of the spin-orbit coupling in orbital degenerated t_{2g} bands in $5d$ transition metal atoms. It is expected that the parallels and differences between the two systems will be elucidated from a more microscopic point of view.

We would like to thank Z. Hiroi, Y. Muraoka, and S. Yonezawa for their help in using the glove box, M. Isobe for his technical assistance, and N. Miyajima, K. Niwa, Y. Taguchi, and T. Katsufuji for enlightening discussions. One of the authors (K.O.) is supported by the Japan Society for the Promotion of Science for Young Scientists.

[1] M. Imada, A. Fujimori, and Y. Tokura, Rev. Mod. Phys. **70**, 1039 (1998).
[2] M. A. Kastner, R. J. Birgeneau, G. Shirane, and Y. Endoh, Rev. Mod. Phys. **70**, 897 (1998).
[3] S. Nakatsuji and Y. Maeno, Phys. Rev. Lett. **84**, 2666 (2000).
[4] F. Kagawa, K. Miyagawa, and K. Kanoda, Nature (London) **436**, 534 (2005).
[5] Y. Takeda, R. Kanno, M. Sakano, O. Yamamoto, M. Takano, Y. Bando, H. Akinaga, H. Takita, and J. B. Goodenough, Mater. Res. Bull. **25**, 293 (1990).
[6] R. J. Cava, B. Batlogg, T. T. Palstra, J. J. Krajewski, W. F. Peck, Jr., A. P. Ramirez, and L. W. Rupp, Jr., Phys. Rev. B **43**, 1229 (1991).
[7] J. Matsuno, Y. Okimoto, M. Kawasaki, and Y. Tokura, Appl. Phys. Lett. **82**, 194 (2003).
[8] V. F. Rodi and D. Babel, Z. Anorg. Allg. Chem. **336**, 17 (1965).
[9] C. L. Mcdaniel and S. J. Schneider, J. Solid State Chem. **4**, 275 (1972).
[10] R. F. Sarkozy, C. W. Moeller, and B. L. Chamberland, J. Solid State Chem. **9**, 242 (1974).
[11] M. Murakami, K. Hirose, K. Kawamura, N. Sata, and Y. Ohishi, Science **304**, 855 (2004).
[12] A. R. Oganov and S. Ono, Nature (London) **430**, 445 (2004).
[13] K. Hirose and Y. Fujita, Geophys. Res. Lett. **32**, L13313 (2005).
[14] N. Miyajima, K. Ohgushi, M. Ichihara, and T. Yagi, Geophys. Res. Lett. **33**, L12302 (2006).
[15] B. G. Hyde, S. Andersson, M. Bakker, C. M. Plug, and M. O'Keefe, Prog. Solid State Chem. **12**, 273 (1979).
[16] K. Kihou, I. Shirotani, Y. Shimaya, C. Sekine, and T. Yagi, Mater. Res. Bull. **39**, 317 (2004).
[17] F. C. Zhang and T. M. Rice, Phys. Rev. B **37**, 3759 (1988).
[18] N. F. Mott, *Metal Insulator Transitions* (Taylor & Francis, London, 1974).
[19] S. Nakatsuji, V. Dobrosavljevic, D. Tanaskovi, M. Minakata, H. Fukazawa, and Y. Maeno, Phys. Rev. Lett. **93**, 146401 (2004).
[20] P. A. Lee and T. V. Ramakrishnan, Rev. Mod. Phys. **57**, 287 (1985).
[21] Y. Ando, G. S. Boebinger, A. Passner, T. Kimura, and K. Kishio, Phys. Rev. Lett. **75**, 4662 (1995).
[22] T. Moriya, *Spin Fluctuations in Itinerant Electron Magnetism* (Springer, New York, 1985).
[23] J. M. Ziman, *Principles of the Theory of Solids*, 2nd ed. (Cambridge University Press, London, 1972).
[24] J. M. Harris, Y. F. Yan, P. Matl, N. P. Ong, P. W. Anderson, T. Kimura, and K. Kitazawa, Phys. Rev. Lett. **75**, 1391 (1995).
[25] T. R. Chien, Z. Z. Wang, and N. P. Ong, Phys. Rev. Lett. **67**, 2088 (1991).
[26] P. W. Anderson, Phys. Rev. Lett. **67**, 2092 (1991).
[27] L. B. Ioffe and A. J. Millis, Phys. Rev. B **58**, 11631 (1998).